Available online freely at www.isisn.org

Bioscience Research

Print ISSN: 1811-9506 Online ISSN: 2218-3973

Journal by Innovative Scientific Information & Services Network

RESEARCH ARTICLE BIOSCIENCE RESEARCH, 2023 20(3):776-781. **OPEN ACCESS**

Effects of hepatic fat and iron deposition on diffusion-weighted images in Magnetic Resonance Imaging

Abujamea H.Abdullah[1], Alsuwailem Lamis[2], Alhaidari Ghadah[2], Alghoraiby Rinad[2], Alshowaiman Reem[1] and Alkubeyyer Metab[1]

[1]Department of Radiology and Medical Imaging, College of Medicine, King Saud University Medical City, King Saud University, Riyadh, **Saudi Arabia**

[2]College of Medicine, King Saud University Medical City, King Saud University, Riyadh, **Saudi Arabia**

***Correspondence: abujamea@ksu.edu.sa** **Received: 17-07-2023, Revised: 05-08-2023, Accepted: 10-08-2023 e-Published: 11-08-2023**

The study aimed to investigate the effects of hepatic fat and iron deposition on the liver's apparent diffusion coefficient (ADC) values in magnetic resonance imaging (MRI). For this purpose, MRI scans of 105 patients with 1.5T scanner of different clinical indications were retrospectively selected and included in the study. A six points-Dixon-based technique called the Iterative decomposition of water and fat with echo asymmetry, and least squares estimation (IDEAL-IQ) was applied to quantify fat and iron deposition level in the liver accurately. Three regions of interest were placed along the posterior right hepatic lobe of the liver, and the relationship between fat fraction and ADC map, fat fraction, and R2* map and ADC and R2* were determined with the Pearson correlation coefficient (r) at a 95% confidence level. The results indicated a weak negative correlation (r=-0.214, p=0.03) but a significant difference between a fat fraction and ADC values. There was no statistically significant (P > 0.05) correlation between fat fraction and the R2* map and between the ADC map and R2* map (r=-0.01, p=0.9), (r=0.05, p=0.58), respectively. The study concluded that an increased hepatic fat fraction decreases ADC measurements on DWI in patients with hepatic diseases with an insignificant effect of hepatic iron overload on ADC values.

Keywords: Magnetic Resonance Imaging, Diffusion-weighted imaging, apparent diffusion coefficient Liver fat fraction, Liver iron overload, liver cirrhosis.

INTRODUCTION

Cirrhosis and liver diseases are known to have a high prevalence and mortality worldwide. Liver diseases account for 2 million deaths annually around the globe, with 1 million deaths per year attributed to cirrhosis, making it the 11th major cause of death in the world, as well as one of the top 20 causes of disability-adjusted life years and years of life lost (Asrani et al. 2019; Fleming et al. 2008). Cirrhosis is characterized by distortion of the hepatic architecture, representing the end stage of chronic liver diseases. Initially, cirrhosis is compensated, and patients are mostly asymptomatic, though, without prompt diagnosis and management, they can deteriorate quickly to a decompensate stage with a 1-year-case fatality rate reaching 80% (Collaborators, 2020). Therefore, detection and management of early-stage fibrosis are vital to hamper the disease's progression and improve prognosis. Liver fibrosis is characterized by collagen, proteoglycans, and other macromolecules built up in the extracellular matrix, a characteristic of all chronic liver disorders. Clinically, liver fibrosis usually develops slowly over decades (Wallace et al. 2008). Liver biopsy remains the gold standard for diagnosing and staging liver fibrosis. However, it is an invasive procedure, is limited by potential complications, and is associated with a high sampling error rate (Janes and Lindor, 1993; Sumida, Nakajima, and Itoh, 2014). Several non-invasive approaches have been explored to evaluate cirrhosis to avoid the limitations of liver biopsy (Sharmaet al. 2014; Wang and Ng, 2011). Diffusion-weighted MRI (DWI) has been proposed as promising (Bonekamp et al. 2011), which is based on image contrast method utilizing microscopic molecular movement of water molecules in the tissues (Baliyan et al. 2016). This technique is becoming more common in standard abdominal MRI protocols (Morani et al. 2013; Saito, Tajima, and Harada, 2016). DWI in the liver allows for identifying and characterizing lesions and assessing diffuse liver diseases (Bharwani and Koh, 2013). The DWI can also be used to identify the stage of cirrhosis with a sensitivity and specificity of 89% and 80%, respectively (Taouli et al. 2007). Since this technique aims to explore the molecular movements of the protons, it is very sensitive and influenced by many confounding variables like fat composition in the tissues and iron overload in the liver (Chandarana et al. 2012).

Therefore, the purpose of this study was to use the

recent advanced techniques of fat measurements in MRI to assess the effect of fat deposition on the MRI apparent diffusion coefficients (ADC). A six points Dixon based technique called Iterative decomposition of water and fat with echo asymmetry and least squares estimation (IDEAL-IQ) sequence (Hines et al. 2011) was employed. The iterative least-squares decomposition algorithm was used to generate maps of the R2* (The reciprocal of T2*) and fat fraction, which provides quantitative estimates of the iron and fat content (Eskreis-Winkler et al. 2018; Hu et al. 2019). IDEAL-IQ sequence is a complex chemical-shift method for fat quantification that accounts for several confounding factors such as T1 bias, eddy currents, noise, and T2* effects (Reeder et al. 2007; Reeder et al. 2005).

MATERIALS AND METHODS

The institutional review board approved the study protocol with a waiver of informed consent due to the study's retrospective nature. The study population consisted of 105 patients who underwent abdominal MRI scans between the 1st of November 2021 and the 28th of February 2022 for different clinical indications. Images of iterative decomposition of water and fat with echo asymmetry and least squares estimation (IDEAL IQ, GE Healthcare) sequence, including fat fraction and R2*, as well as ADC maps generated with (b=0 and b=800) DWI sequence, were collected. All images were acquired from 1.5 Tesla Optima MR450w (GE Healthcare, Milwaukee, WI USA). The imaging protocol includes: an axial breath-hold IDEAL IQ sequence with a repetition time (TR) of 18 ms, effective echo time (TE) of 1.8 ms, flip angle of 8°, the field of view (FOV) of 34-40 cm, a bandwidth of 100 kHz, image matrix of 128 x 128 and slice thickness and spacing were 6 and 2 mm respectively. For the axial diffusion-weighted sequence, a respiratory-gated scan was acquired with the following parameters: repetition time (TR) of 6500 ms, effective echo time (TE) of 63 ms, b-values of 0 and 800, the field of view (FOV) of 34-40 cm, a bandwidth of 100 kHz, image matrix of 128 x 128, slice thickness and spacing were 5 and 2 mm respectively.

Three regions of interest (ROIs) were placed along the posterior right hepatic lobe with a mean size between 180 to 200 mm^2 in the fat fraction map and their corresponding regions in R2* and ADC maps. All ROIs were placed in the liver avoiding liver lesions, major vessels, ligaments, bile ducts, and artifacts, ensuring each ROI was surrounded by liver parenchyma. Images with motion artifacts were excluded. The location of the ROIs in DWI was confirmed to match its counterpart in fat and iron quantification images using the GE advantage windows workstation to synchronize the ROI location in all images. Figure 1 shows the placement of ROIs within the liver.

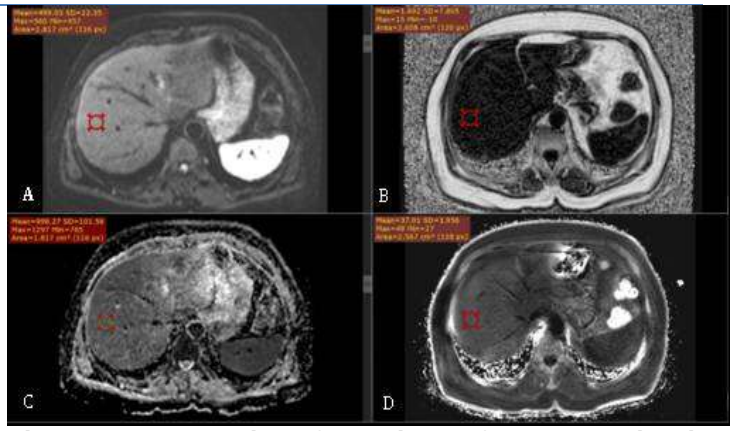

Figure 1: Example of Region of Interest (ROI) placement. A) Diffusion weighted image, B) Fat fraction map, C) ADC map and D) R2* map.

All values are reported as mean ± standard deviation, and a *p*-value of less than 0.05 was considered statistically significant. Microsoft Office Excel 2019 was used on the collected data to apply the Pearson correlation coefficient (*r*) between fat fraction, R2*, and ADC values, as well as the calculation of descriptive statistics. A correlation coefficient measured the strength of the association for absolute values of r where 0-0.19 was regarded as very weak, 0.2-0.39 as weak, 0.40-0.59 as moderate, 0.6-0.79 as strong, and 0.8-1 as very strong correlation, respectively (Campbell, 2021).

RESULTS

The mean age of the patients recruited for the study was 51.8 ± 14.2 (54 females, 51 males). The mean, standard deviation, and range of fat fraction, R2* map, and ADC are presented in Table 1.

Table 1:shows the mean and standard deviations (SD) in addition to the minimum and maximum values of each of the variables of choice.

Variable	Mean	SD	Minimum value	Maximum value
Fat Fraction (%)	10.09	8.36	0.7	34.67
R2* (s^{-1})	34.73	11.8	8.05	70.24
ADC (10^{-3} mm^2/s)	1.039	217.83	686	2042

The mean values of ADC were found to decrease as the fat fraction increased. For liver tissues with a fat fraction of 1%, the mean value of ADC was found to be 1.100 x 10^{-3} mm^2/s compared to 0.900 x 10^{-3} mm^2/s for liver tissues with 34% of the fat fraction. The relationship between fat fraction and ADC values was determined with the Pearson correlation coefficient (r) at a 95% confidence level. Figure 2A highlights a weak negative correlation between fat fraction and ADC values that was statistically significant (*r*=-0.214, *p*=0.03).

On the other hand, liver tissues show no statistically significant correlation between fat fraction and R2* values as well as ADC values and R2* values (*r*=-0.01, *p*=0.9),

(*r*=0.05, *p*=0.58), respectively, as illustrated in figures 2B and 2C.

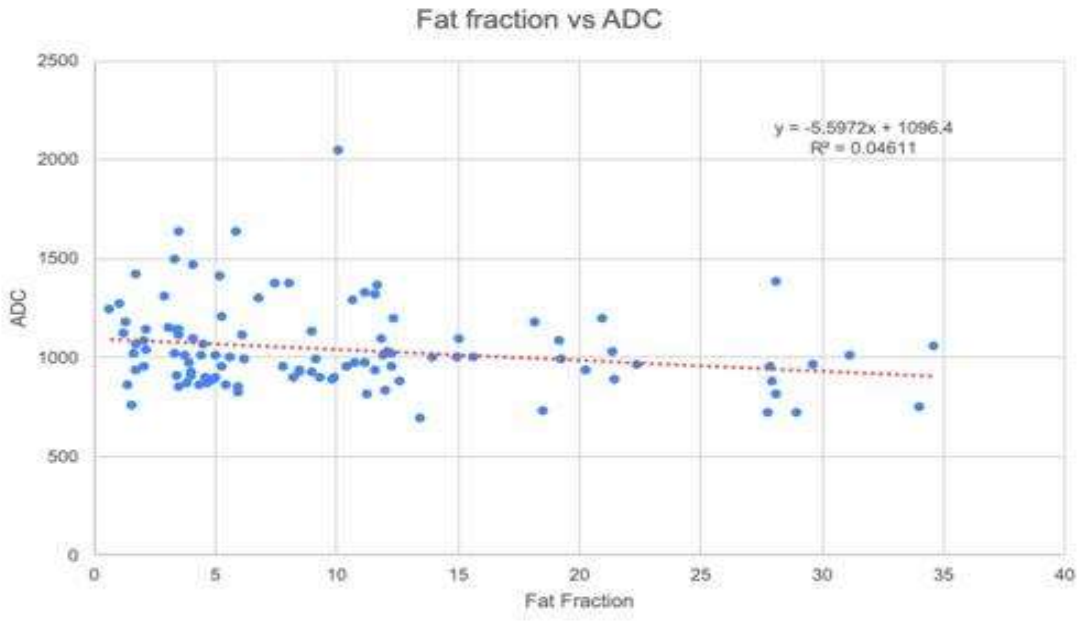

Figure 2A; demonstrates a scatter plot of the Pearson correlation coefficient, with the Y axis representing the ADC map and the X axis representing fat fraction. Correlation is noted throughout the range of values

.

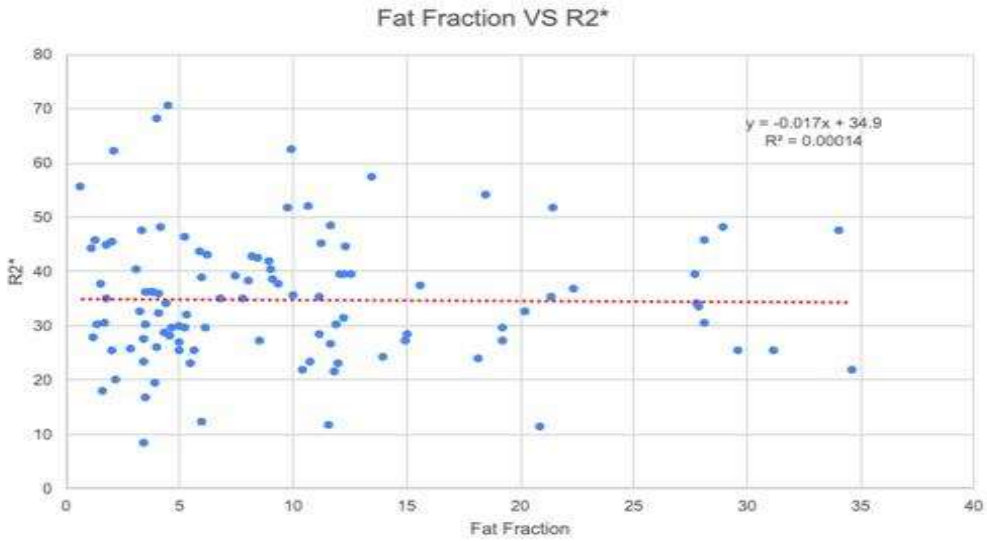

Figure 2B: demonstrates a scatter plot of the Pearson correlation coefficient, with the Y axis representing R2* and the X axis representing fat fraction.
No correlation is noted between the two variables.

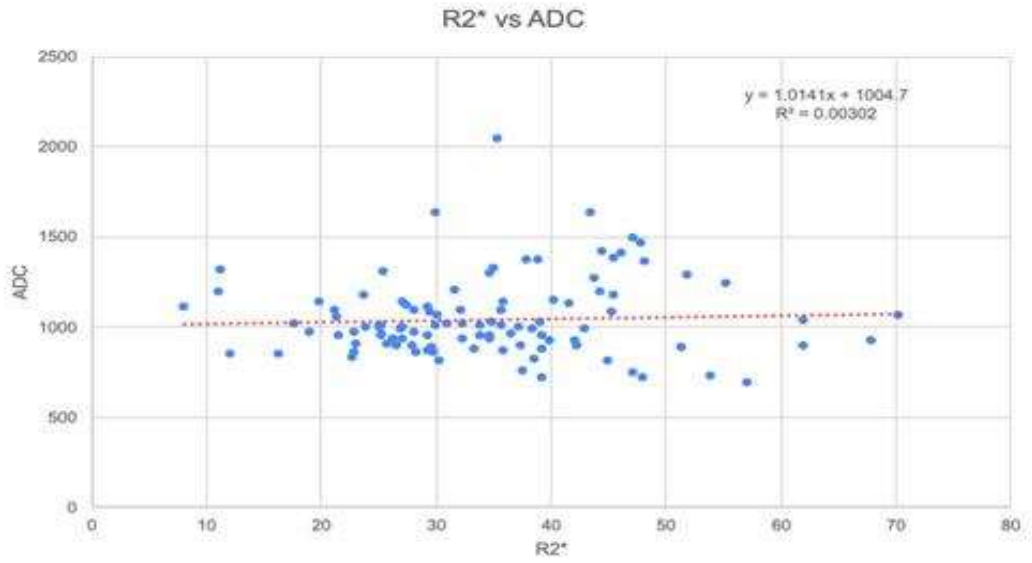

Figure 2C: demonstrates a scatter plot of the Pearson correlation coefficient, with the Y axis representing the ADC map and the X axis representing R2*. No correlation is noted between the two variables.

DISCUSSION

The advancement of magnetic resonance imaging techniques in diagnosing liver diseases allows for identifying and characterizing lesions and assessing diffuse liver diseases, including diffusion-weighted imaging (DWI). In this technique, the image contrast is based on the microscopic molecular movement of water molecules in the tissues. This technique is becoming more common in standard abdominal MRI protocols. Since this technique aims to explore the microscopic molecular movements of the protons, hence is very sensitive and influenced by many confounding variables like fat composition and iron overload in the liver (Bulow et al. 2013).

This study highlighted the correlation between fat fraction and the ADC map. It was observed that there was a weak negative correlation between the two variables, which was consistent with the result obtained in previous literature based on the PDFF and MR spectroscopy that showed a weak correlation between ADC values and PDFF as reported by Makhija et al. (2021)

The traditional MR approach for assessing liver fat, T1-in-and-out-of-phase, fails to identify elevated liver fat in the context of concurrently increased liver iron levels. In the present study, we utilized the Iterative decomposition of water and fat with echo asymmetry and least-squares estimation- iron quantification (IDEAL-IQ) method. This novel MR fat quantification method accounts for various confounding factors, including elevated liver iron (Eskreis-Winkler et al. 2018).

However, results indicated no correlation between the ADC map and the mean iron level, which was consistent with the findings of Kahraman et al. (Kahraman et al. 2022). Unlike a study conducted by Chandarana et al. (2012) on phantom and patients with liver cirrhosis which concluded that hepatic cirrhosis lowers the liver ADC. This contradiction can be explained by the type of sample selected in the study. In our study, we randomly selected the sample among the pool of selected patients that did not necessarily have high iron overload values. This can be considered a limitation of our study. Future studies may be conducted on different categories of patients and different body parts.

Other limitations of this study include obtaining measurements from a single hepatic segment and quantifying the hepatic parenchyma only. Follow-up studies with quantification of the whole liver and correlating hepatic diseases with fat fraction, ADC map, and R2* would be of value.

CONCLUSION

Cirrhosis and liver diseases are known to have a high prevalence and mortality globally. Diffusion-weighted MRI (DWI) has been proposed as a promising technique for evaluating cirrhosis. In this study, we evaluated the effect of liver fat and iron deposition on the accuracy of the diffusion coefficient of the liver. Using the modified six-point Dixion method, fat fraction and iron overload images (R2*) were obtained from the IDEAL-IQ sequence and were correlated to the ADC values obtained from DWI images of the patients. We noticed a weak negative correlation between fat fraction and ADC values that was statistically significant (r=-0.214, p=0.03). No statistically significant correlation was identified between fat fraction and the R2* map as well as the ADC map and R2* star map (r=-0.01, p=0.9), (r=0.05, p=0.58), respectively. In conclusion, our study has shown that increased hepatic fat fraction decreases ADC measurements on DWI in patients

with hepatic diseases. We found no significant effect of hepatic iron overload on ADC values.

CONFLICT OF INTEREST

The authors declared that present study was performed in absence of any conflict of interest.

ACKNOWLEDGEMENT

The authors would like to thank the department of radiology and medical imaging at King Saud University Medical City in Riyadh for their support in offering the data used in this project.

AUTHOR CONTRIBUTIONS

AL, AG, AR and AR was involved in data collection and writing the manuscript. AHJ designed and supervised the project. MK and AHJ reviewed the manuscript. All authors read and approved the final version.

REFERENCES

Asrani, S. K., Devarbhavi, H., Eaton, J., and Kamath, P. S. (2019). Burden of liver diseases in the world. *J Hepatol, 70*(1), 151-171. doi:10.1016/j.jhep.2018.09.014

Baliyan, V., Das, C. J., Sharma, R., and Gupta, A. K. (2016). Diffusion weighted imaging: Technique and applications. *World J Radiol, 8*(9), 785-798. doi:10.4329/wjr.v8.i9.785

Bharwani, N., and Koh, D. M. (2013). Diffusion-weighted imaging of the liver: an update. *Cancer Imaging, 13*(2), 171-185. doi:10.1102/1470-7330.2013.0019

Bonekamp, S., Torbenson, M. S., and Kamel, I. R. (2011). Diffusion-weighted magnetic resonance imaging for the staging of liver fibrosis. *J Clin Gastroenterol, 45*(10), 885-892. doi:10.1097/MCG.0b013e318223bd2c

Bulow, R., Mensel, B., Meffert, P., Hernando, D., Evert, M., and Kuhn, J. P. (2013). Diffusion-weighted magnetic resonance imaging for staging liver fibrosis is less reliable in the presence of fat and iron. *Eur Radiol, 23*(5), 1281-1287. doi:10.1007/s00330-012-2700-2

Chandarana, H., Do, R. K., Mussi, T. C., Jensen, J. H., Hajdu, C. H., Babb, J. S., and Taouli, B. (2012). The effect of liver iron deposition on hepatic apparent diffusion coefficient values in cirrhosis. *AJR Am J Roentgenol, 199*(4), 803-808. doi:10.2214/AJR.11.7541

Collaborators, G. B. D. C. (2020). The global, regional, and national burden of cirrhosis by cause in 195 countries and territories, 1990-2017: a systematic analysis for the Global Burden of Disease Study 2017. *Lancet Gastroenterol Hepatol, 5*(3), 245-266. doi:10.1016/S2468-1253(19)30349-8

Eskreis-Winkler, S., Corrias, G., Monti, S., Zheng, J., Capanu, M., Krebs, S., . . . Mannelli, L. (2018). IDEAL-IQ in an oncologic population: meeting the challenge of concomitant liver fat and liver iron. *Cancer Imaging, 18*(1), 51. doi:10.1186/s40644-018-0167-3

Fleming, K. M., Aithal, G. P., Solaymani-Dodaran, M., Card, T. R., and West, J. (2008). Incidence and prevalence of cirrhosis in the United Kingdom, 1992-2001: a general population-based study. *J Hepatol, 49*(5), 732-738. doi:10.1016/j.jhep.2008.05.023

Hines, C. D., Frydrychowicz, A., Hamilton, G., Tudorascu, D. L., Vigen, K. K., Yu, H., . . . Reeder, S. B. (2011). T(1) independent, T(2) (*) corrected chemical shift based fat-water separation with multi-peak fat spectral modeling is an accurate and precise measure of hepatic steatosis. *J Magn Reson Imaging, 33*(4), 873-881. doi:10.1002/jmri.22514

Hu, F., Yang, R., Huang, Z., Wang, M., Yuan, F., Xia, C., . . . Song, B. (2019). 3D Multi-Echo Dixon technique for simultaneous assessment of liver steatosis and iron overload in patients with chronic liver diseases: a feasibility study. *Quantitative Imaging in Medicine and Surgery, 9*(6), 1014-1024.

Janes, C. H., and Lindor, K. D. (1993). Outcome of patients hospitalized for complications after outpatient liver biopsy. *Ann Intern Med, 118*(2), 96-98. doi:10.7326/0003-4819-118-2-199301150-00003

Kahraman, A. S., Kahraman, B., Ozdemir, Z. M., Karaca, L., Sahin, N., and Yilmaz, S. (2022). Diffusion-weighted imaging of the liver in assessing chronic liver disease: effects of fat and iron deposition on ADC values. *Eur Rev Med Pharmacol Sci, 26*(18), 6620-6631. doi:10.26355/eurrev_202209_29762

Makhija, N., Vikram, N. K., Srivastava, D. N., and Madhusudhan, K. S. (2021). Role of Diffusion-Weighted Magnetic Resonance Imaging in the Diagnosis and Grading of Hepatic Steatosis in Patients With Non-alcoholic Fatty Liver Disease: Comparison With Ultrasonography and Magnetic Resonance Spectroscopy. *J Clin Exp Hepatol, 11*(6), 654-660. doi:10.1016/j.jceh.2021.02.008

Morani, A. C., Elsayes, K. M., Liu, P. S., Weadock, W. J., Szklaruk, J., Dillman, J. R., . . . Hussain, H. K. (2013). Abdominal applications of diffusion-weighted magnetic resonance imaging: Where do we stand. *World J Radiol, 5*(3), 68-80. doi:10.4329/wjr.v5.i3.68

Reeder, S. B., McKenzie, C. A., Pineda, A. R., Yu, H., Shimakawa, A., Brau, A. C., . . . Brittain, J. H. (2007).

Water-fat separation with IDEAL gradient-echo imaging. *J Magn Reson Imaging, 25*(3), 644-652. doi:10.1002/jmri.20831

Reeder, S. B., Pineda, A. R., Wen, Z., Shimakawa, A., Yu, H., Brittain, J. H., . . . Pelc, N. J. (2005). Iterative decomposition of water and fat with echo asymmetry and least-squares estimation (IDEAL): application with fast spin-echo imaging. *Magn Reson Med, 54*(3), 636-644. doi:10.1002/mrm.20624

Saito, K., Tajima, Y., and Harada, T. L. (2016). Diffusion-weighted imaging of the liver: Current applications. *World J Radiol, 8*(11), 857-867. doi:10.4329/wjr.v8.i11.857

Sharma, S., Khalili, K., and Nguyen, G. C. (2014). Non-invasive diagnosis of advanced fibrosis and cirrhosis. *World J Gastroenterol, 20*(45), 16820-16830. doi:10.3748/wjg.v20.i45.16820

Sumida, Y., Nakajima, A., and Itoh, Y. (2014). Limitations of liver biopsy and non-invasive diagnostic tests for the diagnosis of nonalcoholic fatty liver disease/nonalcoholic steatohepatitis. *World J Gastroenterol, 20*(2), 475-485. doi:10.3748/wjg.v20.i2.475

Taouli, B., Tolia, A. J., Losada, M., Babb, J. S., Chan, E. S., Bannan, M. A., and Tobias, H. (2007). Diffusion-weighted MRI for quantification of liver fibrosis: preliminary experience. *AJR Am J Roentgenol, 189*(4), 799-806. doi:10.2214/AJR.07.2086

Wallace, K., Burt, A. D., and Wright, M. C. (2008). Liver fibrosis. *Biochem J, 411*(1), 1-18. doi:10.1042/BJ20071570

Wang, Y. X., and Ng, C. K. (2011). The impact of quantitative imaging in medicine and surgery: Charting our course for the future. *Quant Imaging Med Surg, 1*(1), 1-3. doi:10.3978/j.issn.2223-4292.2011.09.01